# Dynamic Specification of a Reference Point for Hypervolume Calculation in SMS-EMOA

Hisao Ishibuchi
Department of Computer Science and Engineering
Southern University of Science and Technology (SUSTech)
Shenzhen, China
hisao@sustc.edu.cn

Ryo Imada, Naoki Masuyama and Yusuke Nojima
Department of Computer Science and Intelligent Systems
Osaka Prefecture University
Sakai, Osaka 599-8531, Japan
{ryo.imada@ci., masuyama@, nojima@}cs.osakafu-u.ac.jp

***Abstract*—The hypervolume has been frequently used as an indicator to compare the performance of evolutionary multi-objective optimization (EMO) algorithms. It has also been used in indicator-based algorithms (e.g., SMS-EMOA and HypE). In such an EMO algorithm, a multi-objective problem is handled as a single-objective problem to maximize the hypervolume of a pre-specified number of solutions. Whereas a reference point is needed for hypervolume calculation, its specification has not been discussed in detail in many studies. This may be because the reference point specification has almost no effect on experimental results when hypervolume-based EMO algorithms are applied to frequently-used scalable test problems such as DTLZ and WFG with triangular Pareto fronts. However, when the Pareto front of a test problem is not triangular (e.g., minus-DTLZ and minus-WFG), the reference point specification has a dominant effect on solution sets obtained by hypervolume-based EMO algorithms. In this paper, first we explain the importance of an appropriate reference point specification in SMS-EMOA. Then we examine the use of a dynamically changing specification of the reference point in SMS-EMOA.**

***Keywords—Hypervolume, reference point, indicator-based algorithms, SMS-EMOA, evolutionary multi-objective optimization.***

## I. Introduction

Evolutionary multi-objective optimization (EMO) has been a very active research area in the last two decades in the field of evolutionary computation. A number of EMO algorithms have been proposed in the literature. Those algorithms are often categorized into three classes: Pareto dominance-based (e.g., SPEA [1], NSGA-II [2]), decomposition-based (e.g., C-MOGA [3], MOEA/D [4]) and indicator-based (e.g., IBEA [5] and MaOEA/IGD [6]). Each class of algorithms has its own advantages and disadvantages. Pareto dominance-based has been the most popular class since Goldberg's suggestion in 1989 [7]. One of the disadvantages of this class is a severe decrease in the selection pressure towards the Pareto front by the increase in the number of objectives [8]. Decomposition-based algorithms relatively work well on many-objective problems. However, their performance usually strongly depends on the shape of the Pareto front [9].

In indicator-based EMO algorithms, the hypervolume [10] has been frequently used as an indicator (e.g., SMS-EMOA [11] and HypE [12]). The use of the hypervolume has a clear theoretical support: The hypervolume is a Pareto compliant performance indicator [13]. High performance of SMS-EMOA and HypE on many-objective problems has been reported in the literature [12], [14]. One difficulty of hypervolume-based EMO algorithms is their large computation load, especially for many-objective problems.

A reference point is needed for hypervolume calculation. Calculated hypervolume values of solution sets directly depend on the location of the reference point. However, its appropriate specification has not been discussed in detail in the EMO community. A common practice is to use a little bit worse reference point than the nadir point. There exists no widely-accepted specific numerical guideline about the location of the reference point. As a result, a variety of different specifications have been used for performance comparison in the literature. For example, the reference point for DTLZ1 [15] was specified as a point inferior to the nadir point by 1% in Seada & Deb [16], 10% in Yuan et al. [17] and Maltese et al. [18], 40% in Wagner et al. [14], and 100% in Li et al. [19]. In Zhang et al. [20], the nadir point itself was used as the reference point.

When multi-objective test problems have triangular Pareto fronts such as DTLZ1-4 [15] and WFG4-9 [21], the location of the reference point does not have a large effect on performance comparison results [22], [23]. For those test problems (and also for most two-objective test problems [24]), the location of the reference point has almost no effect on the optimal distribution of solutions for hypervolume maximization as far as the reference point is worse than the nadir point. As a result, the location of the reference point in hypervolume-based EMO algorithms such as SMS-EMOA does not have a large effect on solution sets obtained for those test problems. This may be the reason why an appropriate reference point specification has not been discussed for hypervolume-based EMO algorithms in detail. For example, the reference point in SMS-EMOA is simply specified by adding 1 to the worst objective value of each objective among the individuals in the current population. When the current population is a good approximation of the true Pareto front of a multi-objective minimization problem with the ideal point (0, 0, ..., 0) and the nadir point (1, 1, ..., 1) such as DTLZ2-4 and WFG4-9, this specification corresponds to the 100% worse specification than the nadir point.

Recently, it has been pointed out in Ishibuchi et al. [22], [23] that the location of the reference point has a large effect on the optimal distribution of solutions for multi-objective test

This work was supported by the Science and Technology Innovation Committee Foundation of Shenzhen (Grant No. ZDSYS201703031748284).

978-1-5090-6017-7/18/$31.00 ©2018 IEEE

problems with inverted triangular Pareto fronts (e.g., minus-DTLZ1-4 [9] and minus-WFG4-9 [9]) and some other test problems with complicated Pareto fronts (e.g., WFG3 with a partially degenerate Pareto front [25]). This suggests that the location of the reference point for those test problems may have a large effect on performance comparison results of EMO algorithms. This also suggests that the search behavior of hypervolume-based EMO algorithms may strongly depend on the specification of the reference point. In this paper, we examine the dependency of obtained solution sets by SMS-EMOA on the reference point specification. Especially, we examine the usefulness of a dynamically changing method of the reference point where we gradually decrease the distance between the reference point and the estimated nadir point during the execution of SMS-EMOA. In this method, the reference point gradually approaches to the final target location, which is specified by the estimated nadir point, the population size and the number of objectives. Through computational experiments, it is shown that this approach is useful for some test problems. However, our experimental results also show the difficulty of hypervolume-based EMO algorithms to find a set of well-distributed solutions for some other test problems independent of the specification of the reference point.

This paper is organized as follows: First, we briefly explain the hypervolume and the SMS-EMOA in Section II. Next, in Section III, we explain the dependency of the optimal distribution of solutions for hypervolume maximization on the location of the reference point for multi-objective problems with triangular and inverted triangular Pareto fronts. Then, we report our experimental results of SMS-EMOA with various specification methods of the reference point in Section IV. Our experiments are performed on the three-objective DTLZ1-2 [15], minus-DTLZ1-2 [9], and distance minimization problems [26] for visually examining the obtained solution sets by SMS-EMOA. Finally, we conclude this paper in Section V.

## II. Multi-Objective Optimization and SMS-EMOA

### A. Multi-Objective Optimization Problem

In this paper, we assume that we have the following $m$-objective minimization problem:

$$\text{Minimize } \boldsymbol{f}(\boldsymbol{x}) = (f_1(\boldsymbol{x}), ..., f_m(\boldsymbol{x})) \text{ subject to } \boldsymbol{x} \in \mathbf{X}, \quad (1)$$

where $\boldsymbol{f}(\boldsymbol{x})$ is an $m$-dimensional objective vector, $f_i(\boldsymbol{x})$ is the $i$th objective to be minimized ($i = 1, 2, ..., m$), $\boldsymbol{x}$ is the decision vector, and $\mathbf{X}$ is the feasible region.

### B. Hypervolume

For the multi-objective problem in (1), the task of EMO algorithms is to search for a pre-specified number of non-dominated solutions which approximate the entire Pareto front as good as possible. This means that we need to evaluate the approximation quality of different solution sets for comparing different EMO algorithms. The hypervolume [10], which is defined as the area, volume or hypervolume of the dominated region by a solution set (see Fig. 1 (a)), is the most frequently-used performance indicator in the EMO community. As shown in Fig. 1 (a), we need the reference point $\boldsymbol{r}$ in the objective space in order to calculate the hypervolume (i.e., to bound the dominated region by the solution set in the objective space). Fig. 1 (b) explains the hypervolume contribution of each solution, which is defined by the decrease in the hypervolume value by removing each solution from the solution set.

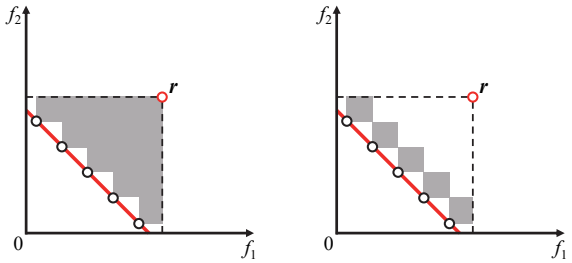


(a) Hypervolume. (b) Hypervolume contribution.

Fig. 1. Explanations of the hypervolume and the hypervolume contribution. The red line shows the Pareto front, the five open circles on the red line are solutions, and the red circle $\boldsymbol{r}$ is the reference point.

### C. SMS-EMOA

SMS-EMOA [11] is a hypervolume-based EMO algorithm with a ($\mu$+1) generation update mechanism. A new individual is generated and added to the current population, and the worst individual is removed. This algorithm tries to maximize the hypervolume of a population of $\mu$ individuals by iterating the ($\mu$+1) generation update mechanism. The basic idea of the generation update mechanism in SMS-EMOA is to remove a single worst individual with the least hypervolume contribution from the enlarged population of ($\mu$+1) individuals. This is the same as choosing the best set of $\mu$ individuals with the largest hypervolume from the ($\mu$+1) individuals.

## III. Optimal Distribution of Solutions

In this section, we explain the dependency of the optimal distribution of solutions for hypervolume maximization on the location of the reference point. SMS-EMOA is used to search for the optimal distribution of solutions for test problems with various shapes of the Pareto fronts. In this paper, the $m$-dimensional objective space is normalized so that the ideal and nadir points become (0, 0, ..., 0) and (1, 1, ..., 1), respectively. For the simplicity of explanations, the reference point $\boldsymbol{r}$ is specified as $\boldsymbol{r}$ = ($r$, $r$, ..., $r$) by a single real number $r$. For example, $r$ = 2 means that the reference point $\boldsymbol{r}$ is specified as (2, 2, ..., 2), which is 100% worse than the nadir point (1, 1, ..., 1) in the normalized objective space.

In this section, the normalization of the objective space is performed using the true ideal point and the true nadir point in order to search for the optimal distribution of solutions for each test problem and each specification of the reference point. That is, we assume that the true ideal point and the true nadir point are known for each test problem. In the next section, the normalization is performed using the estimated ideal and nadir points which are updated in each population of SMS-EMOA. The estimated ideal point is defined by the best value of each objective among all solutions in each population while the estimated nadir point is defined by the worst value of each objective among non-dominated solutions in each population in the next section.

In our computational experiments in this section, we do not use distance variables in DTLZ1-2 and minus-DTLZ1-2. That is, the number of distance variables is always specified as zero. Under this setting, we can focus on the search for the optimal distribution of solutions since all feasible solutions are on the Pareto front. For each test problem, we apply SMS-EMOA many times and calculate the hypervolume of the obtained solution sets for all specifications of the reference point. Then we report the best result for each specification as the obtained approximate optimal distribution of solutions.

### *A. Optimal Distributions of Solutions: Two-Objective Cases*

For two-objective problems, the optimal distribution of solutions for hypervolume maximization was theoretically discussed in Auger et al. [24]. When the Pareto front is linear, the hypervolume is maximized by a set of equally-spaced solutions. When the Pareto front is non-linear, the optimal distribution of solutions depends on the slope of the Pareto front. The region of the Pareto front with the slope of 45 degree has the highest solution density (for details, see [24]).

In Figs. 2-4, we show the obtained approximate optimal distributions of six solutions for a different Pareto front (which is shown by the grey line or curve in each figure) and a different specification of the reference point. In each figure, we examine three specifications of the reference point: $r$ = 1 (the same as the nadir point), $r$ = 1.2 (20% worse than the nadir point) and $r$ = 10. The population size in SMS-EMOA is specified as six. As we have already explained, the objective space of each test problem is normalized in Figs. 2-4.

When the reference point is the nadir point in (a), the two extreme solutions of the Pareto front have no hypervolume contribution. As a result, these two points are not included in the optimal distribution in each figure. However, the three distributions in (a)-(c) in each figure are similar to each other whereas the location of the reference point is totally different. This is because the location of the reference point has an effect only on the hypervolume contributions of the top-left and bottom-right solutions in the solution set. We can also see from Figs. 2-4 that the shape of the Pareto front has a large effect on the optimal distribution of solutions.

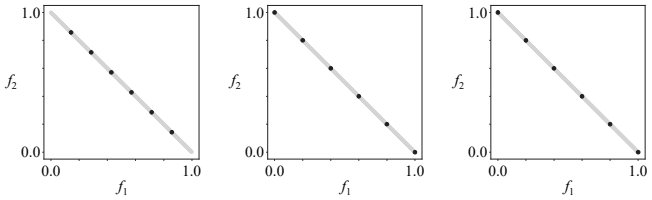


(a) $r$ = 1. (b) $r$ = 1.2. (c) $r$ = 10.

Fig. 2. Optimal distributions for the two-objective DTLZ1.

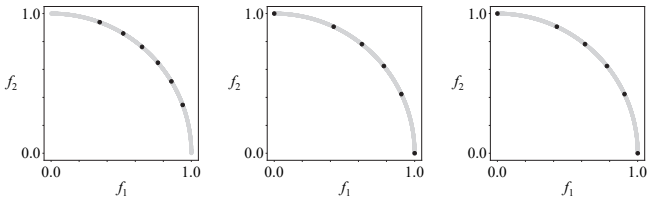


(a) $r$ = 1. (b) $r$ = 1.2. (c) $r$ = 10.

Fig. 3. Optimal distributions for the two-objective DTLZ2.

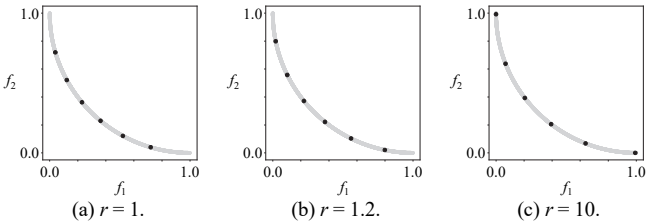


(a) $r$ = 1. (b) $r$ = 1.2. (c) $r$ = 10.

Fig. 4. Optimal distributions for the two-objective minus-DTLZ2.

### *B. Optimal Distribution of Solutions: DTLZ*

In Fig. 5, we show the obtained approximate optimal distributions of 21 solutions for the three-objective DTLZ1 problem. The population size in SMS-EMOA is specified as 21. In Fig. 5 (a) where the nadir point is used as the reference point, the three extreme (i.e., corner) solutions of the Pareto front are not included in the obtained distribution of solutions since their hypervolume contributions are zero. Whereas the reference point specifications are totally different in Fig. 5 (a)-(c), the distribution of solutions for each specification is similar to each other. This is because the location of the reference point has an effect only on the hypervolume contributions of the three extreme solutions on the corners of the Pareto front when those solutions are included in the solution set as in Fig. 5 (b) and (c).

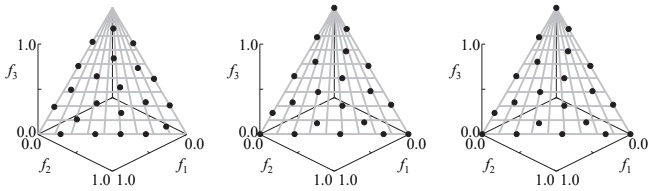


(a) $r$ = 1. (b) $r$ = 1.2. (c) $r$ = 10.

Fig. 5. Optimal distributions for the three-objective DTLZ1.

In Fig. 6, we show the obtained approximate optimal distributions of 21 solutions for the three-objective DTLZ2 problem. As in Fig. 5, the three extreme solutions on the corners of the Pareto front are not included in the obtained distribution of solutions in Fig. 6 (a) whereas they are included in Fig. 6 (b) and (c). However, the obtained distributions of solutions in Fig. 6 (a)-(c) are similar to each other. Our experimental results in Figs. 2-6 clearly show that the shape of the Pareto front (i.e., linear, concave or convex) has a much larger effect than the location of the reference point on the optimal distribution of solutions. This observation suggests that the location of the reference point does not have a large effect on hypervolume-based comparison results of EMO algorithms or experimental results of hypervolume-based EMO algorithms. This may be the reason why the location of the reference point has not been discussed in detail in the literature.

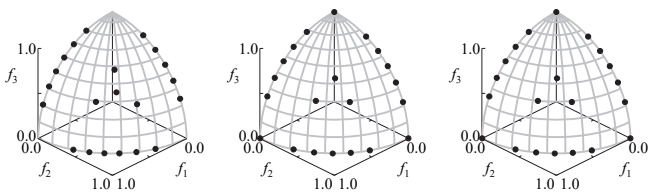


(a) $r$ = 1. (b) $r$ = 1.2. (c) $r$ = 10.

Fig. 6. Optimal distributions for the three-objective DTLZ2.

### C. Optimal Distribution of Solutions: minus-DTLZ

In Fig. 7, we show the obtained approximate optimal distribution of solutions for the three-objective minus-DTLZ1 problem. In Fig. 7 (a), no solutions on the boundary of the inverted triangular Pareto front are included in the obtained distribution of solutions. This is because all of those solutions have no hypervolume contribution when the nadir point is used as the reference point for the inverted triangular Pareto front (for details, see [22]). When $r$ = 1.2 in Fig. 7 (b), the optimal distribution of solutions is a well-distributed solution set over the entire Pareto front as in Fig. 5 for the three-objective DTLZ1. However, when $r$ = 10 (i.e., the reference point is far away from the nadir point) in Fig. 7 (c), all solutions are on the boundary of the Pareto front. This is because those solutions have much larger hypervolume contributions than any inside solutions when the reference point is far away from the nadir point (for details, see [22]). In the case of the triangular Pareto front, only the three extreme solutions have much larger hypervolume contributions. The comparison between Fig. 5 and Fig. 7 clearly shows that the effect of the location of the reference point on the optimal distribution of solutions strongly depends on the problem. When the Pareto front is inverted triangular, the location of the reference point has a large effect on the optimal distribution of solutions.

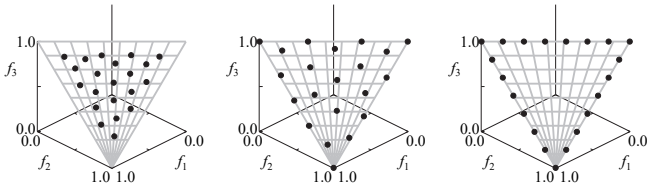


(a) $r$ = 1. (b) $r$ = 1.2. (c) $r$ = 10.

Fig. 7. Optimal distributions for the three-objective minus-DTLZ1.

In Fig. 8, we show the obtained approximate optimal distribution of solutions for the three-objective minus-DTLZ2 problem. As in Fig. 7 (a), no solutions close to the sides of the inverted triangular Pareto front are included in the obtained distribution of solutions in Fig. 8 (a) when the nadir point is used as the reference point. On the contrary, when the reference point is far away from the nadir point in Fig. 8 (c), almost all solutions are very close to the boundary of the Pareto front. However, since the shape of the Pareto front is convex, those solutions are not on the boundary of the Pareto front in Fig. 8 (c) (see Fig. 4 for the effect of the convex Pareto front). Our experimental results in Fig. 8 suggest the difficulty of obtaining a well-distributed solution set over the entire Pareto front of the minus-DTLZ2 problem by SMS-EMOA independent of the location of the reference point. The same difficulty can be also observed in Fig. 6 for DTLZ2.

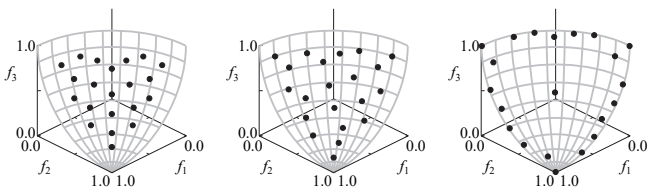


(a) $r$ = 1. (b) $r$ = 1.2. (c) $r$ = 10.

Fig. 8. Optimal distributions for the three-objective minus-DTLZ2.

## IV. Reference Point Specification for SMS-EMOA

### A. Reference Point Specification Methods

Recently, a reference point specification method was proposed for fair performance comparison in Ishibuchi et al. [22], [23]. The basic idea is to specify the reference point so that uniformly distributed solutions over the entire Pareto front have similar hypervolume contributions. This idea is explained in the case of a linear Pareto front in Fig. 9. In Fig. 9 (a), the two extreme solutions have smaller hypervolume contributions than the inside four solutions since the reference point is too close to the nadir point. On the contrary, in Fig. 9 (c), the two extreme solutions have much larger hypervolume contributions than the inside four solutions since the reference points is too far from the nadir point. Only when $r$ = 1.2 in Fig. 9 (b), all solutions have the same hypervolume contribution.

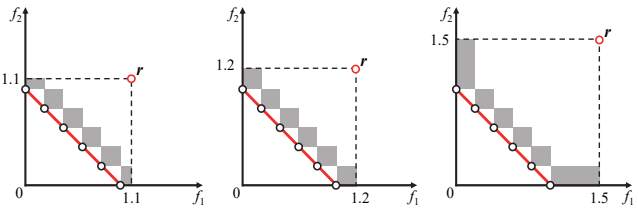


(a) $r$ = 1.1. (b) $r$ = 1.2. (c) $r$ = 1.5.

Fig. 9. Hypervolume contribution of each solution.

Let us denote the population size by $\mu$. When solutions are uniformly distributed on the entire linear Pareto front as in Fig. 9, the Pareto front is divided into $H = \mu - 1$ intervals of the same width ($H$ = 5 in Fig. 9). In this case, each solution has the same hypervolume contribution only when the reference point $\boldsymbol{r} = (r, r)$ is specified as $r = 1 + (1/H)$ as shown in Fig. 9 (b).

In general, $H$ is the number of divisions of each side of the Pareto front, which is the same as the integer parameter $H$ in MOEA/D used for generating uniformly distributed weight vectors. In MOEA/D, the number of weight vectors (i.e., the population size $\mu$) is calculated from the number of objectives $m$ and the integer parameter $H$ as $\mu = C_{m-1}^{H+m-1}$. Using this formulation, the value of $H$ is specified in the reference point specification method as follows [22], [23]:

$$C_{m-1}^{H+m-1} \le \mu < C_{m-1}^{H+m} . \quad (2)$$

The reference point $\boldsymbol{r} = (r, r, ..., r)$ is specified as $r = 1 + (1/H)$ in the normalized objective space where the ideal and nadir points are (0, 0, ..., 0) and (1, 1, ..., 1), respectively.

This reference point specification method was proposed for hypervolume-based performance comparison where the Pareto front of each test problem was known. In its application to SMS-EMOA, we estimate the ideal and nadir points from the current population to normalize the objective space as follows: the ideal and nadir points are estimated as the best and worst objective values of each objective among the non-dominated solutions in the current population. After normalizing the objective space using the estimated ideal and nadir points, we specified the reference point $\boldsymbol{r} = (r, r, ..., r)$ as $r = 1 + (1/H)$ in each generation of SMS-EMOA.

The estimated ideal and nadir points from the non-dominated solutions in each generation are not close to the true ideal and nadir points especially in early generations. As a result, the normalization based on the estimated ideal and nadir points often has unexpected bad effects on the search behavior of EMO algorithms [27]. In order to decrease such an unexpected bad effect of the inaccurate estimation of the ideal and nadir points, we use a larger (i.e., worse) value of $r$ than the suggested value $r = 1 + (1/H)$ in early generations. More specifically, we specify the reference point at the $t$th generation as follows:

$$r(t) = r_{Initial}\frac{(T-t)}{T} + (1+1/H)\frac{t}{T}, \quad t = 0, 1, ..., T, \qquad (3)$$

where $T$ is the total number of generations, and $r_{Initial}$ is the initial value of $r$, which is larger than $1 + (1/H)$. In (3), the value of $r$ gradually approaches to the suggested specification in [22], [23]. The initial value $r_{Initial}$ is specified as $r_{Initial} = 2$ in this paper. In our computational experiments, we examine various specifications of the reference point in SMS-EMOA including the proposed idea in (3), the suggested specification $1 + (1/H)$ in [22], [23], the nadir point $r = 1$, and some other fixed specifications of $r$: $r = 1.1$, 2, and 10.

### B. Setting of Computational Experiments

SMS-EMOA is applied to the three-objective DTLZ1-2, minus-DTLZ1-2 and distance minimization problems under the following conditions:

Population size: 55 ($H = 9$),
Number of solution evaluations: 100,000 solutions,
Crossover: SBX (distribution index: 20),
Crossover probability: 1.0,
Mutation: Polynomial mutation (distribution index: 20),
Mutation probability: $1/n$ ($n$: the number of variables),
Number of variables ($n$): 7 (DTLZ1 and minus-DTLZ1)
12 (DTLZ1 and minus-DTLZ2)
10 (distance minimization),
Number of runs: 5.

Since $H$ is calculated as $H = 9$ from the population size 55, the suggested reference point in [22], [23] is $r = 10/9$. Among experimental results from five runs for each reference point specification, we select the result with the median hypervolume value as the representative result in this paper.

### C. Experimental Results on DTLZ

Experimental results on the three-objective DTLZ1 are shown in Fig. 10. Except for the case of $r = 1$ in Fig. 10 (a) where the estimated nadir point is used as the reference point, very similar results are obtained in Fig. 10 (b)-(f). When the estimated nadir point is used as the reference point, the extreme solutions among the non-dominated solutions in the current population have no hypervolume contribution. If all solutions are non-dominated in the current population, one of the extreme solutions is removed from the current population by the $(\mu + 1)$ generation update mechanism of SMS-EMOA. As a result, the diversity of solutions gradually decreases throughout the execution of SMS-EMOA. Thus the diversity of the final population is very small in Fig. 10 (a). Except for Fig. 10 (a), good results are obtained in Fig. 10 (b)-(f) independent of the choice of a reference point specification method.

Fig. 11 shows experimental results on the three-objective DTLZ2. As in Fig. 10, very similar results are obtained in Fig. 11 except for the case of $r = 1$ in Fig. 11 (a). Experimental results in Fig. 10 and Fig. 11 suggest that the reference point specification is not important as long as the reference point is not too close to the estimated nadir point.

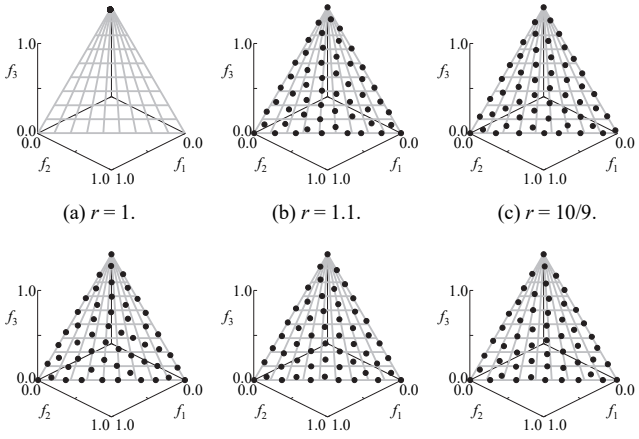


(a) $r = 1$. (b) $r = 1.1$. (c) $r = 10/9$.

(d) $r = 2$. (e) $r = 10$. (f) $r = 2$ to $10/9$.

Fig. 10. Experimental results by SMS-EMOA on DTLZ1.

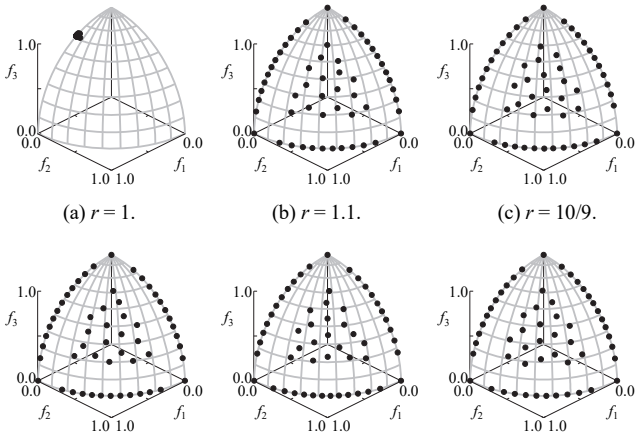


(a) $r = 1$. (b) $r = 1.1$. (c) $r = 10/9$.

(d) $r = 2$. (e) $r = 10$. (f) $r = 2$ to $10/9$.

Fig. 11. Experimental results by SMS-EMOA on DTLZ2.

### D. Experimental Results on minus-DTLZ

Experimental results on the three-objective minus-DTLZ1 are shown in Fig. 12. When $r = 1$ (i.e., the estimated nadir point is used as the reference point) in Fig. 12 (a), the diversity of the obtained solutions is very small as in Fig. 10 and Fig. 11. All solutions in Fig. 12 (a) are around the center of the Pareto front. On the contrary, when $r = 10$, almost all the solutions are on the boundary of the Pareto front. Only when the reference point is appropriately specified in Fig. 12 (b), (c) and (f), the obtained solutions uniformly cover the entire Pareto front. Our experimental results in Fig. 12 show the importance of the reference point specification in SMS-EMOA. However, we

cannot observe any advantage of the dynamically changing specification in Fig. 12 (f) over the pre-specified specifications in Fig. 12 (b) and (c).

Fig. 13 shows experimental results on the three-objective minus-DTLZ2. As in Figs. 10-12, good results are not obtained from $r = 1$ in Fig. 13 (a). When the reference point is far away from the nadir point in Fig. 13 (e) with $r = 10$, almost all the solutions are close to the boundary of the Pareto front. When $r = 2$ in Fig. 13 (d), the obtained solutions cover the entire Pareto front. However, the density of solutions around the boundary of the Pareto front is much higher than that around the center. In Fig. 13 (b), (c) and (f), the distributions of solutions around the center of the Pareto front are denser and more uniform than those in Fig. 13 (d) and (e). However, no solutions are obtained around the boundary of the Pareto front. Our experimental results in Fig. 13 (and also in Fig. 11) show the difficulty of finding uniformly distributed solutions over the entire Pareto front by SMS-EMOA when the Pareto front is non-linear.

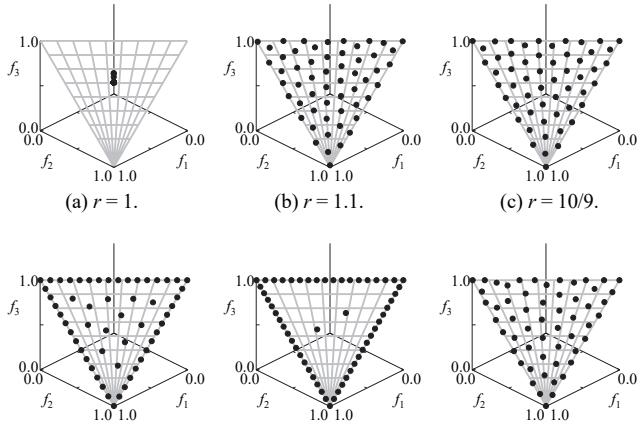


Fig. 12. Experimental results by SMS-EMOA on minus-DTLZ1.

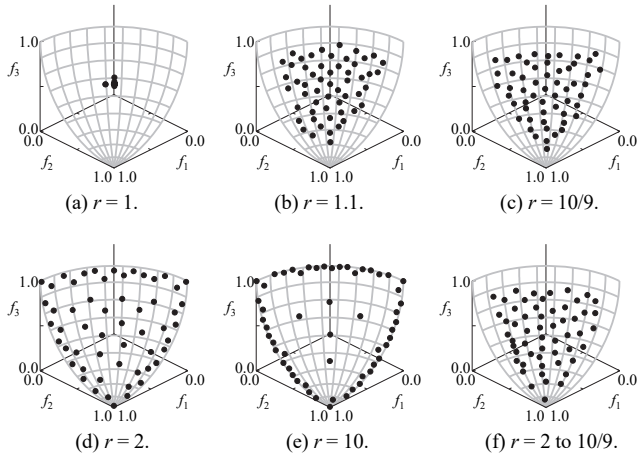


Fig. 13. Experimental results by SMS-EMOA on minus-DTLZ2.

With respect to the comparison between Fig. 13 (c) and Fig. 13 (f), we can see that the diversity of the obtained solutions is slightly larger in Fig. 13 (f) than Fig. 13 (c). This is because the diversity of solutions increases in early generations where the reference point is far away from the nadir point.

### *E. Experimental Results on Distance Minimization Problem*

In order to further examine the positive effect of the dynamically changing reference point on the diversity of solutions, we apply SMS-EMOA to a multi-objective distance minimization problem [26]. First, we specify three points A, B and C in the 10-dimensional decision space $[0, 100]^{10}$ as follows: A = (25, 25, ..., 25), B = (75, 25, 75, 25, ..., 75, 25), C = (25, 75, 25, 75, ..., 25, 75). Each objective of our three-objective distance minimization problem is to minimize the distance to each point. The Pareto optimal solution set is the inside and the boundary of the triangle ABC in the 10-dimensional decision space $[0, 100]^{10}$. Experimental results are shown in Fig. 14 (in the $f_2$-$f_3$ space, which is a projection from the three-dimensional objective space) and Fig. 15 (in the $x_1$-$x_2$ space, which is a projection from the 10-dimensional decision space).

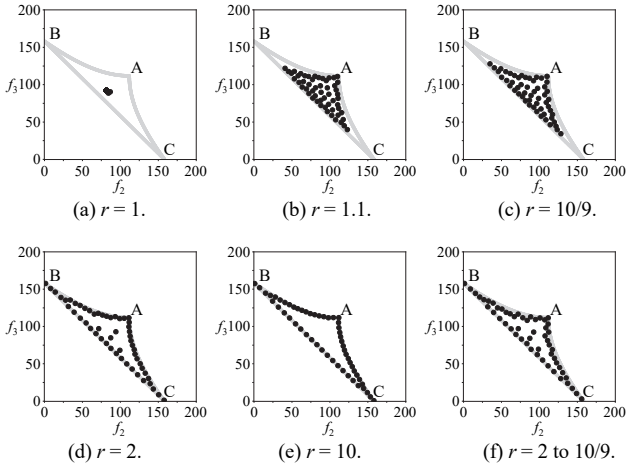


Fig. 14. Experimental results on the three-objective ten-dimensional distance minimization problem in the $f_2$-$f_3$ space.

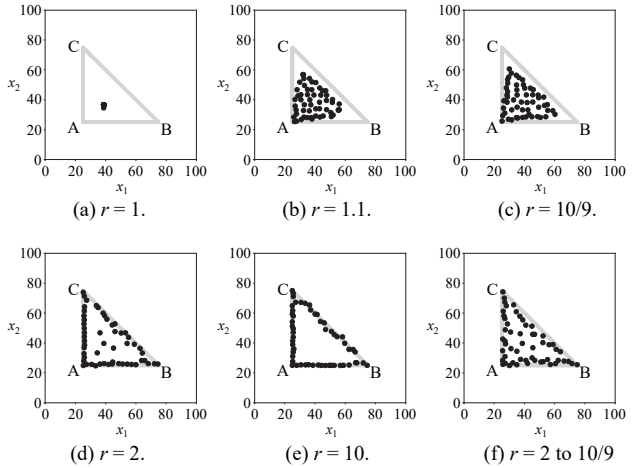


Fig. 15. Experimental results on the three-objective ten-dimensional distance minimization problem in the $x_1$-$x_2$ space.

In Fig. 14 and Fig. 15, when $r = 1$ in (a), the diversity of the obtained solutions is very small as in Figs. 10-13. When $r = 2$

in (d) and $r = 10$ in (e), almost all solutions are close to the boundary of the Pareto front. When $r = 1.1$ in (b) and 10/9 in (c), no solutions are obtained around Point B and Point C. However, by dynamically changing the specification of the reference point from $r = 2$ to $r = 10/9$ during the execution of SMS-EMOA in (f), solutions around all the three points A, B, and C are obtained together with more inside solutions than the case of $r = 2$. This observation suggests the potential usefulness of the dynamically changing reference point.

The comparison between (b) and (c) in Fig. 14 and Fig. 15 shows that a very small difference in the value of $r$ (i.e., the difference between $r = 1.1$ and $r = 10/9$: $1/90 = 10/9 - 1.1$) leads to a visible difference in the obtained solution sets. This observation suggests the importance of the reference point specification in SMS-EMOA.

## V. Concluding Remarks

In this paper, we examined the reference point specification in SMS-EMOA. Through computational experiments, we obtained the following observations.

(1) For all test problems used in this paper, the diversity of the obtained solutions was very small when the estimated nadir point was used as the reference point. The estimated nadir point was specified by the worst value of each objective among the non-dominated solutions in the current population.

(2) For DTLZ1-2 with the triangular Pareto fronts, almost the same results were obtained from various specifications of the reference point (except for the use of the estimated nadir point). This observation suggests that the reference point specification in SMS-EMOA is not important for test problems with triangular Pareto fronts.

(3) For minus-DTLZ1-2, totally different solution sets were obtained from different specifications of the reference point. When the reference point was far away from the nadir point, almost all solutions were obtained around the boundary of the Pareto front. Only when the reference point was appropriately specified, the entire Pareto front was covered by the obtained solutions. This observation suggests that the reference point specification in SMS-EMOA is very important for test problems with inverted triangular Pareto fronts.

(4) For DTLZ2 and minus-DTLZ2, obtained solutions were not uniformly distributed over the entire Pareto fronts independent of the choice of a reference point specification method. This observation suggests the difficulty of obtaining the uniformly distributed solutions for test problems with non-linear Pareto fronts by hypervolume-based EMO algorithms.

(5) The proposed dynamically changing method of the reference point showed a promising result for the three-objective 10-dimensional distance minimization problem. This observation suggests the potential usefulness of the proposed method for difficult multi-objective problems.

Our experimental results clearly explained that the effect of the location of the reference point on the search behavior of SMS-EMOA strongly depends on the problem. In the past, the performance of SMS-EMOA (and other EMO algorithms) on many-objective problems has been mainly examined through computational experiments on the DTLZ and WFG test problems with triangular Pareto fronts in the literature. Thus the importance of the reference point specification in SMS-EMOA (and also for performance comparison of EMO algorithms for many-objective optimization) was not well recognized in the EMO community. We hope that our experimental results in this paper will motivate further studies on the reference point specification for hypervolume calculation.

## References


[1] E. Zitzler and L. Thiele, "Multiobjective evolutionary algorithms: A comparative case study and the strength Pareto approach," *IEEE Trans. on Evolutionary Computation*, vol. 3, no. 4, pp. 257-271, Nov. 1999.

[2] K. Deb, A. Pratap, S. Agarwal, and T. Meyarivan, "A fast and elitist multiobjective genetic algorithm: NSGA-II," *IEEE Trans. on Evolutionary Computation*, vol. 6, no. 2, pp. 182-197, April 2002.

[3] T. Murata, H. Ishibuchi, and M. Gen, "Specification of genetic search directions in cellular multi-objective genetic algorithm," *Lecture Notes in Computer Science 1993: Evolutionary Multi-Criterion Optimization* - EMO 2001, pp. 82-95, Springer, Berlin, March 2001.

[4] Q. Zhang and H. Li, "MOEA/D: A multiobjective evolutionary algorithm based on decomposition," *IEEE Trans. on Evolutionary Computation*, vol. 11, no. 6, pp. 712-731, December 2007.

[5] E. Zitzler and S. Künzli, "Indicator-based selection in multiobjective search," *Lecture Notes in Computer Science 3242: Parallel Problem Solving from Nature - PPSN VIII*, pp. 832-842, Springer, Berlin, September 2004.

[6] Y. Sun, G. G. Yen, and Z. Yi, "IGD indicator-based evolutionary algorithm for many-objective optimization problems," *IEEE Trans. on Evolutionary Computation*, Early Access Paper, 2018.

[7] D. E. Goldberg, *Genetic Algorithms in Search, Optimization, and Machine Learning*, Addison-Wesley, Reading, MA, 1989

[8] H. Ishibuchi, N. Akedo, and Y. Nojima, "Behavior of multi-objective evolutionary algorithms on many-objective knapsack problems," *IEEE Trans. on Evolutionary Computation*, vol. 19, no. 2, pp. 264-283, April 2015.

[9] H. Ishibuchi, Y. Setoguchi, H. Masuda, and Y. Nojima, "Performance of decomposition-based many-objective algorithms strongly depends on Pareto front shapes," *IEEE Trans. on Evolutionary Computation*, vol. 21, no. 2, pp. 169-190, April 2017.

[10] E. Zitzler and L. Thiele, "Multiobjective optimization using evolutionary algorithms – A comparative case study," *Lecture Notes in Computer Science 1498: Parallel Problem Solving from Nature - PPSN V*, pp. 292-301, Springer, Berlin, September 1998.

[11] N. Beume, B. Naujoks, and M. Emmerich, "SMS-EMOA: Multiobjective selection based on dominated hypervolume," *European Journal of Operational Research*, vol. 181, no. 3, pp. 1653-1669, September 2007.

[12] J. Bader and E. Zitzler, "HypE: An algorithm for fast hypervolume-based many-objective optimization," *Evolutionary Computation*, vol. 19 no. 1, pp. 45-76, Spring 2011.

[13] E. Zitzler, D. Brockhoff, and L. Thiele, "The hypervolume indicator revisited: On the design of Pareto-compliant indicators via weighted integration," *Lecture Notes in Computer Science 4403: Evolutionary Multi-Criterion Optimization - EMO 2007*, pp. 862-876, Springer, Berlin, March 2007.

[14] T. Wagner, N. Beume, and B. Naujoks, "Pareto-, aggregation-, and indicator-based methods in many-objective optimization," *Lecture Notes in Computer Science 4403: Evolutionary Multi-Criterion Optimization - EMO 2007*, Springer, Berlin (2007) 742-756.

[15] K. Deb, L. Thiele, M. Laumanns, and E. Zitzler, "Scalable multi-objective optimization test problems," *Proc. of 2002 IEEE Congress on Evolutionary Computation*, pp. 825-830, May 12-17, 2002.

[16] H. Seada and K. Deb, "A unified evolutionary optimization procedure for single, multiple, and many objectives," *IEEE Trans. on Evolutionary Computation*, vol. 20, no. 3, pp. 358-369, June 2016.

[17] Y. Yuan, H. Xu, B. Wang, and X. Yao, "A new dominance relation based evolutionary algorithm for many-objective optimization," *IEEE Trans. on Evolutionary Computation*, vol. 20, no. 1, pp. 16-37, February 2016.

[18] J. Maltese, B. M. Ombuki-Berman, and A. P. Engelbrecht, "A scalability study of many-objective optimization algorithms," *IEEE Trans. on Evolutionary Computation* (Early Access Paper: Available from IEEE Xplore).

[19] K. Li, K. Deb, Q. Zhang, and S. Kwong, "An evolutionary many-objective optimization algorithm based on dominance and decomposition," *IEEE Trans. on Evolutionary Computation*, vol. 19, no. 5, pp. 694-716, October 2015.

[20] X. Zhang, Y. Tian, R.Cheng, and Y. Jin, "A decision variable clustering-based evolutionary algorithm for large-scale many-objective optimization," *IEEE Trans. on Evolutionary Computation*, vol. 22, no. 1, pp. 97-112, Feb. 2018.

[21] S. Huband, P. Hingston, L. Barone, and L. While, "A review of multiobjective test problems and a scalable test problem toolkit," *IEEE Trans. on Evolutionary Computation*, vol. 10, no. 5, pp. 477-506, October 2006.

[22] H. Ishibuchi, R. Imada, Y. Setoguchi, and Y. Nojima, "Hypervolume subset selection for triangular and inverted triangular Pareto fronts of three-objective problems," *Proc. of 14th ACM/SIGEVO Conference on Foundations of Genetic Algorithms* (FOGA 2017), pp. 95-110, Copenhagen, Denmark, January 12-15, 2017.

[23] H. Ishibuchi, R. Imada, Y. Setoguchi, and Y. Nojima, "Reference point specification in hypervolume calculation for fair comparison and efficient search," *Proc. of 2017 Genetic and Evolutionary Computation Conference*, pp. 585-592, Berlin, Germany, July 15-19, 2017.

[24] A. Auger, J. Bader, D. Brockhoff, and E. Zitzler, "Hypervolume-based multiobjective optimization: Theoretical foundations and practical implications," *Theoretical Computer Science*, vol. 425, pp. 75-103, March 2012.

[25] H. Ishibuchi, H. Masuda, and Y. Nojima, "Pareto fronts of many-objective degenerate test problems," *IEEE Trans. on Evolutionary Computation*, vol. 20, no. 5, pp. 807-813, October 2016.

[26] H. Ishibuchi, M. Yamane, N. Akedo, and Y. Nojima, "Many-objective and many-variable test problems for visual examination of multiobjective search," *Proc. of 2013 IEEE Congress on Evolutionary Computation*, pp. 1491-1498, Cancún, México, June 20-23, 2013.

[27] H. Ishibuchi, K. Doi, and Y. Nojima, "On the effect of normalization in MOEA/D for multi-objective and many-objective optimization," *Complex & Intelligent Systems*, vol. 3, no. 4, pp. 279–294, Dec 2017.